NATURAL RESOURCES PROGRAM

SPACE APPLICATIONS PROGRAMS

TECHNICAL LETTER NASA-20

U.S. Geological Survey
Department of the Interior

UNITED STATES
DEPARTMENT OF THE INTERIOR
GEOLOGICAL SURVEY
WASHINGTON, D.C. 20242

Technical Letter
NASA-20
July 1966

Dr. Peter C. Badgley
Chief, Natural Resources Program
Office of Space Science and Applications
Code SAR, NASA Headquarters
Washington, D.C. 20546

Dear Peter:

Transmitted herewith are 3 copies of:

TECHNICAL LETTER NASA-20

COMPOSITION OF BASALT FLOWS AT PISGAH

CRATER, CALIFORNIA: PRELIMINARY DATA*

by

Jules D. Friedman**

Sincerely yours,

William A. Fischer
Research Coordinator for
USGS/NASA Natural Resources Program

*Work performed under NASA Contract No. R-146
**U.S. Geological Survey, Washington, D.C.

U. S. Government Agencies Only

UNITED STATES

DEPARTMENT OF THE INTERIOR

GEOLOGICAL SURVEY

TECHNICAL LETTER NASA-20

COMPOSITION OF BASALT FLOWS AT PISGAH CRATER, CALIFORNIA: PRELIMINARY DATA*

by

Jules D. Friedman

These data are preliminary and should not be quoted without permission.

*Work performed under NASA Contract No. R-146

Prepared by the Geological Survey
for the National Aeronautics and
Space Administration (NASA)

TABLE OF CONTENTS

LIST OF TABLES

LIST OF ILLUSTRATIONS

LIST OF ILLUSTRATIONS (CON'T)

INTRODUCTION

Compositional analyses of the surface of a pahoehoe flow of porphyritic olivine basalt of eruptive phase three and the surface of an aa flow of porphyritic olivine basalt of eruptive phase two of Pisgah Volcano, were carried out as part of a series of geologic studies undertaken in 1965 in the Pisgah Crater area, San Bernardino County, California, in connection with a study of airborne infrared survey data.

Infrared imagery recording the radiance in the 8-13μ range from the terrestrial surface is in good spatial agreement with conventional aerial photography and geologic field mapping (Wise, 1966, and Gawarecki, oral communication) on the position of the contact between basalt flows of eruptive phase two and phase three. Infrared image tonal density and surface radiance (Fischer et al., 1965) recorded on the ground at the time of the IR airborne survey indicate the radiance from phase two is slightly greater than phase three in pre-dawn hours.

Sampling grids were 225 feet^2; samples of basalt exposed at the surface were taken from the 16 nodes of each grid. Sampling grid P-1 is located 1200 feet S57W of VABM 2543 (high point of Pisgah Crater), T.8N, R.6E, Section 32; sampling grid P-2 is located 1250 feet S13W of VABM 2543, T.8N, R.6E, Section 32; Lavic Lake, California Quadrangle, 1:62,500, USGS.

Analyses of a single sample of each of the two lithologies were made by several methods to determine if compositional variations between the two basalt flows are great enough, particularly at the weathered surface, to justify a program of statistical sampling and analysis. This is a report of findings on these analyses.

ACKNOWLEDGMENTS

Rapid rock analyses for major elements were made by Paul Elmore, Sam Botts and Lowell Artis with Leonard Shapiro as Project Leader; semiquantitative spectrographic analyses for minor elements were carried out by Joseph L. Harris with Armin W. Helz as Project Leader. Electron probe microanalyses and electron scanning photomicrographs were made by Cynthia W. Mead and conventional photomicrographs of polished sections were taken by Tony Denson. All analytical work and photography was performed in the laboratories of the Geological Survey except petrographic modal analyses which were made at the University of California, Santa Barbara, by William S. Wise. The field team which carried out sample grid selection, lithologic sampling and ground radiometry during airborne infrared surveys in February 1965, included David L. Daniels, William A. Fischer, Stephen J. Gawarecki, William R. Hemphill and the author.

LITHOLOGY OF PISGAH BASALT FLOWS

Eruptive Phase Two (sampling grid P-2)

The basalt flows of the eruptive phase two are largely aa - textured; the basalt is porphyritic with olivine (2-3mm) and plagioclase (2-5mm) phenocrysts. Groundmass minerals are generally the same as earlier and later flows.

Eruptive Phase Three (sampling grid P-1)

The flow surface of the eruptive phase three is entirely pahoehoe-textured, though pressure ridges and tumuli are common. Plagioclase phenocrysts larger than 10mm and clots of olivine crystals about 5-6mm across distinguish these flows from the earlier ones (Wise, 1966).

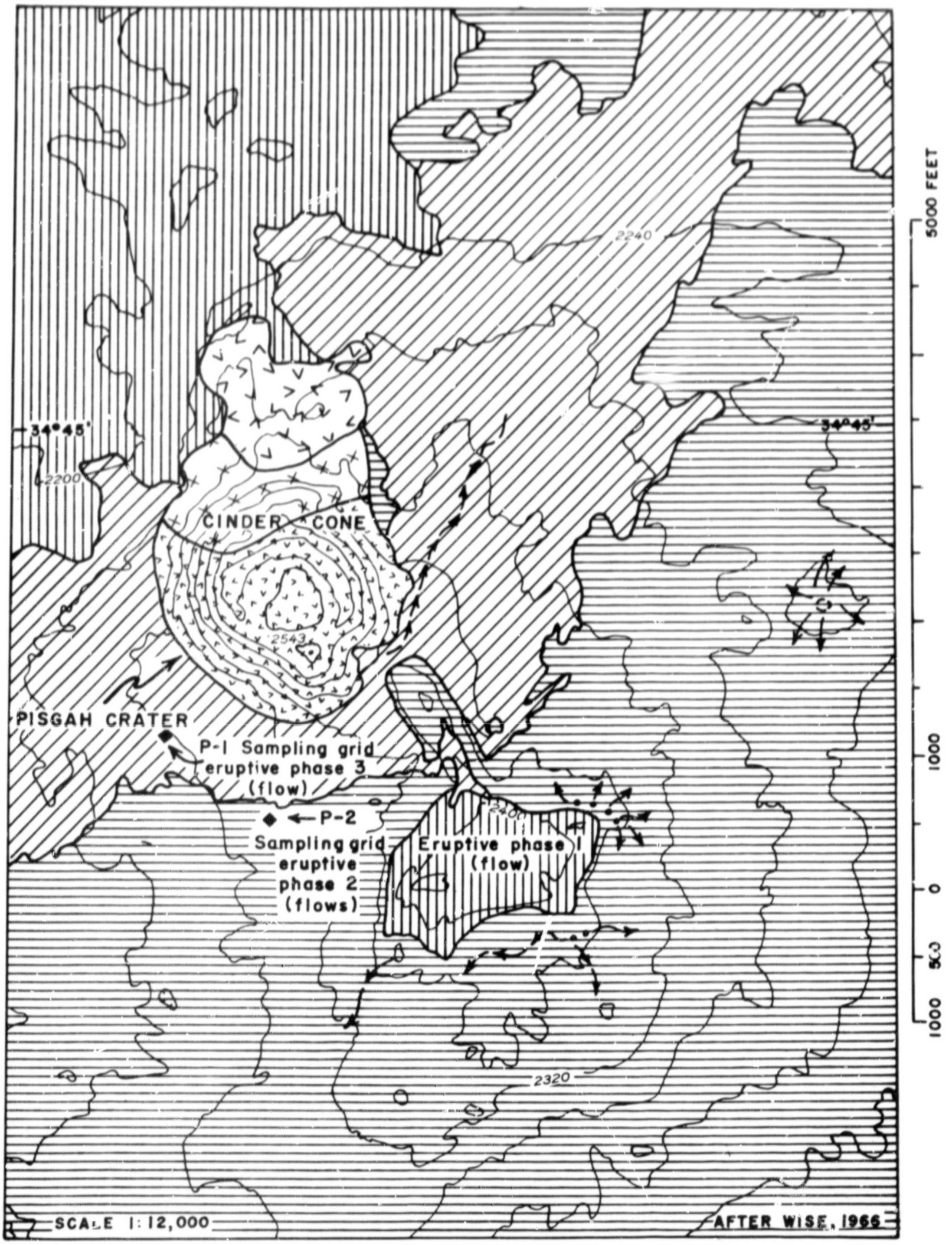

PLATE 1. Location of sampling grids P-1 and P-2, Pisgah lavas

EXPLANATION FOR GEOLOGIC MAP OF THE PISGAH LAVAS,
SAN BERNARDINO COUNTY, CALIFORNIA

Pisgah Lavas

CINDERS

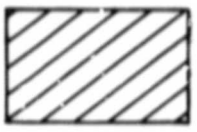

FLOWS

Porphyritic olivine basalt of eruptive phase three

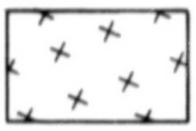

CINDERS

FLOWS

Porphyritic olivine basalt of eruptive phase two

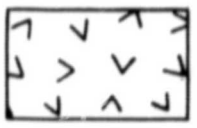

CINDERS

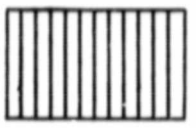

FLOWS

Microporphyritic olivine basalt of eruptive phase one

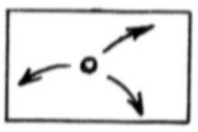

Lava vent, with flow directions of last flow on surface

Modal Analyses*

By

William S. Wise

An average of eight 2000-point counts each were made on petrographic thin sections cut from surface samples of grids P-1 and P-2, Pisgah flows.

Minerals	Flow two (P-2, aa)	Flow three (P-1 pahoehoe)
olivine		
phenocrysts	3.5	1.5
groundmass	2.2	2.8
plagioclase		
phenocrysts	2.8	4.4
groundmass	11.9	12.2
clinopyroxene		
phenocrysts	0.0	0.2
groundmass	3.7	0.6
alkali feldspar	0.7	12.2
opaques	tr	tr
apatite	tr	tr
glass	41.9	48.4
voids	34.0	30.0

*Note the low degree of crystallization in analyzing these modal analyses; P-1 and P-2 are at least 75% glass and bubbles.

ELECTRON PROBE MICROANALYSIS FOR SURFACE COMPOSITION

Analysis by Cynthia W. Mead

Compositional variations of the weathered surfaces of P1-3D (pahoehoe-textured porphyritic olivine basalt of eruptive phase three) and P2-3B (aa-textured porphyritic olivine basalt of eruptive phase two) were analyzed with the electron probe by utilizing polished sections cut transverse to the natural rock surface thus exposing the weathered surface layers and fresh inner material of the basalt.

The areas chosen for analysis were on the periphery of the samples and extended a short distance in toward the center. In both samples, two bands were noted on the periphery. These two bands consisted of a fairly wide light gray band which will be referred to as the outer band and a narrow bright, almost metallic band which will be referred to as the inner band. The main mass or inner material will be referred to as the matrix. The bands range in thickness from about 15μ to 120μ.

After coating the polished specimens submitted for analysis with carbon in order to make their surfaces electrically conducting, the following types of analysis were made:

A. Complete spectrometer traces were made in order to determine the elements present.

B. Counts were taken on the outer band, inner band, and the matrix for the elements present. These counts were qualitative in nature; they were compared only with each other and not with standards.

C. Spectrometer scans were made across the outer band, inner band, and matrix for the elements present by moving the specimen under the electron beam while the spectrometers were positioned for a given element. These scans supplemented the information gained by method B and D.

D. X-ray and specimen current pictures were taken on the oscilloscope screens. Photomicrographs were taken of the areas scanned while the X-ray and specimen current pictures were being taken.

Analytical Results

Both samples were analyzed for their Mg, Fe, Al, Ti and Si content and in both samples, distinct differences in the concentration of Fe, Al, Ti, Si and to a slight extent Mg could be noted in the outer band, inner band and the matrix.

The data collected by making counts, scans, and taking X-ray photographs is summarized in Table I.

TABLE I

Relative elemental concentration of Al, Fe, Si, Ti* in P1-3D and P2-3B as shown by:

Electron Probe Microanalysis

Sample	Al	Fe	Si	Ti	Area of Sample
P1-3D	2	2	1	2	Matrix
	3	1	3	1	Inner Band
	1	3	2	3	Outer Band
P2-3B	1	2	1	2	Matrix
	3	1	3	1	Inner Band
	2	3	2	3	Outer Band

1 area of highest concentration
2 area of intermediate concentration
3 area of lowest concentration

* Mg is not included because the differences were barely discernible.

A visual representation of the data is afforded by two groups of photographs. The first group is a series of scanning photographs taken on the oscilloscope screen of the electron probe. The specimen current photographs show differences in current across the sample; light areas indicate reduction of current caused by the concentration of elements of high atomic number; dark areas indicate an increase in current caused by the concentration of elements of low atomic number. The electron probe scanning photographs show concentrations of white dots registered on a collecting screen by characteristic X-radiation engendered by the impingement of an electron beam on a polished sample. The X-ray spectrometer is set for characteristic spectral lines and thus registers the differential concentration of specific elements. Figures 9-13 in the first group of photographs were taken in the same general area of P1-3D as were figures 4-8 but the sample was rotated

180° in order to make sure that the differences in composition were real and not due to an edge effect. The material designated as the outer band appears to be part of the mounting medium. However this is apparently not the case because the elemental differences indicated by electron probe microanalysis are reproducible and remained the same regardless of the orientation of the sample. Also, the specimen current remained stable while on that part of the sample whereas it was not stable when it was on the mounting medium -- in fact the beam burned holes in it.

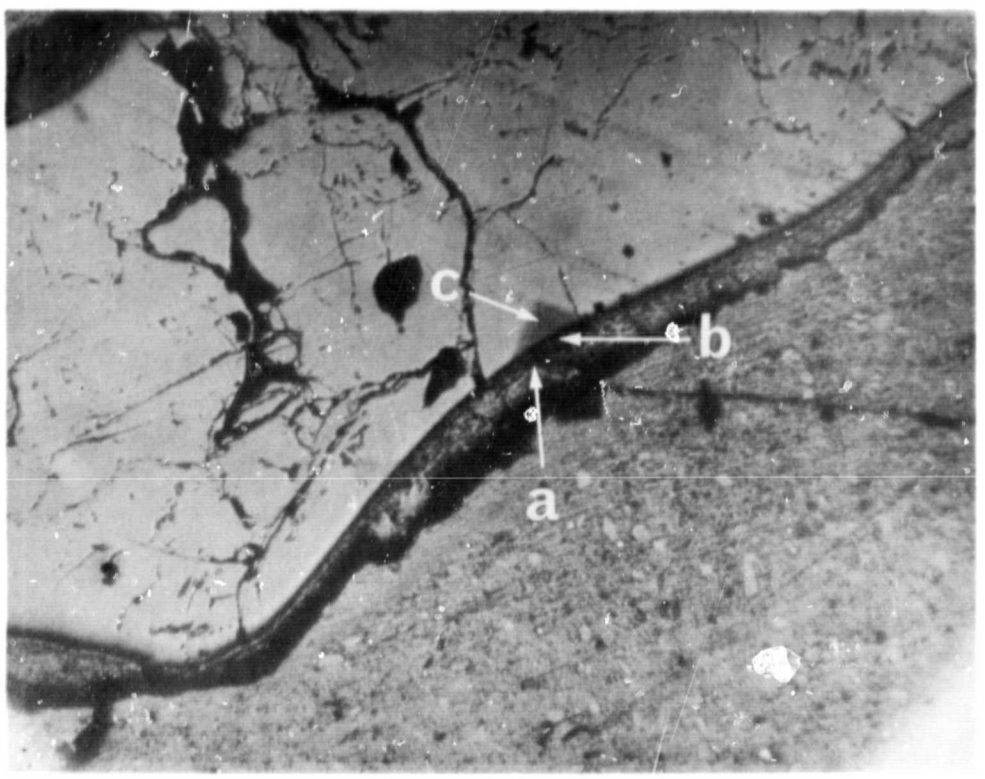

Fig. 1 - Photomicrograph of P1-3D (pahoehoe) showing two scanned areas. Darker scanned area is where scanning photographs figures 4-8 were taken. Lighter scanned area is where scanning photographs figures 9-13 were taken after 180° rotation of the specimen. Three series of white dots, visible only in the matrix* but actually extending to the edge of the specimen, and appearing above the second scanned area, mark location of point by point traverses made to determine elemental variation in the specimen. x42

*The fairly wide light gray band (a) is referred to as the "outer band." The narrow, bright, almost metallic band (b) is referred to as the "inner band." The main mass or inner material (c) of the polished section is referred to as the "matrix."

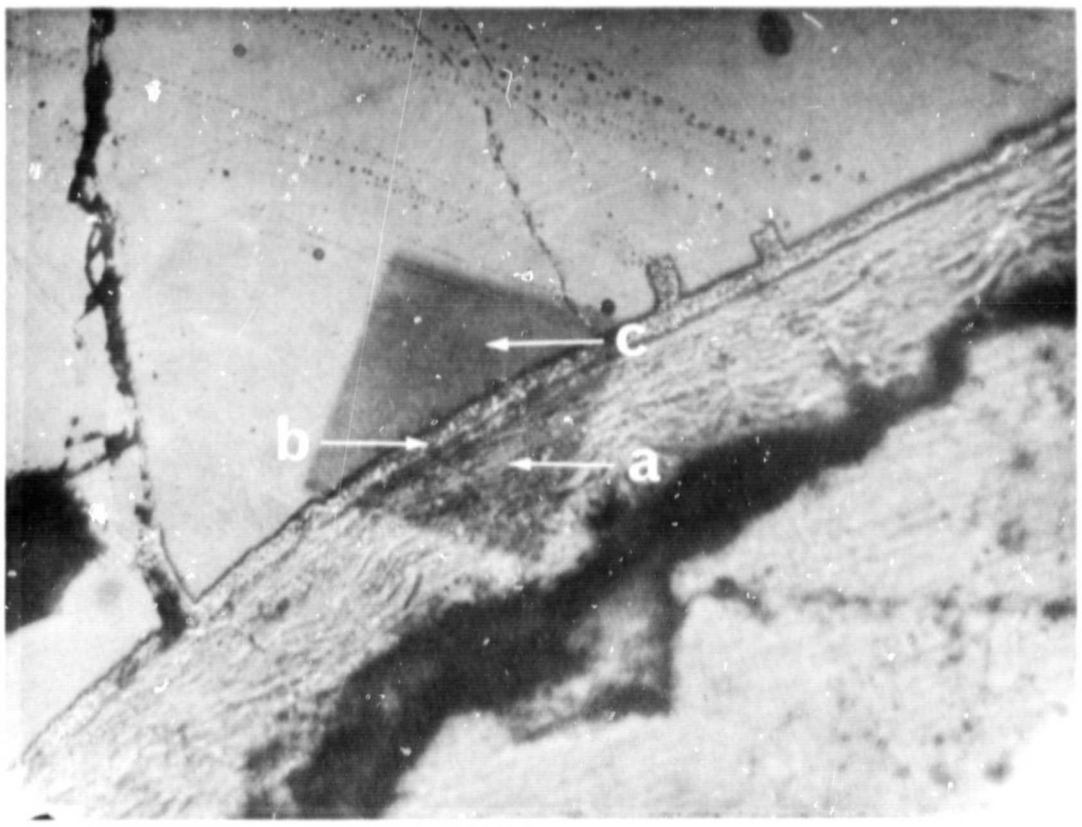

Fig. 2 - Section P1-3D.Pahoehoe lava. Enlarged photomicrograph of the scanned area where electron probe scanning photographs figures 4-8 were taken. Outer band (a) is about 120μ thick; inner band (b) is 15μ thick. Matrix (c) is at the top. x160

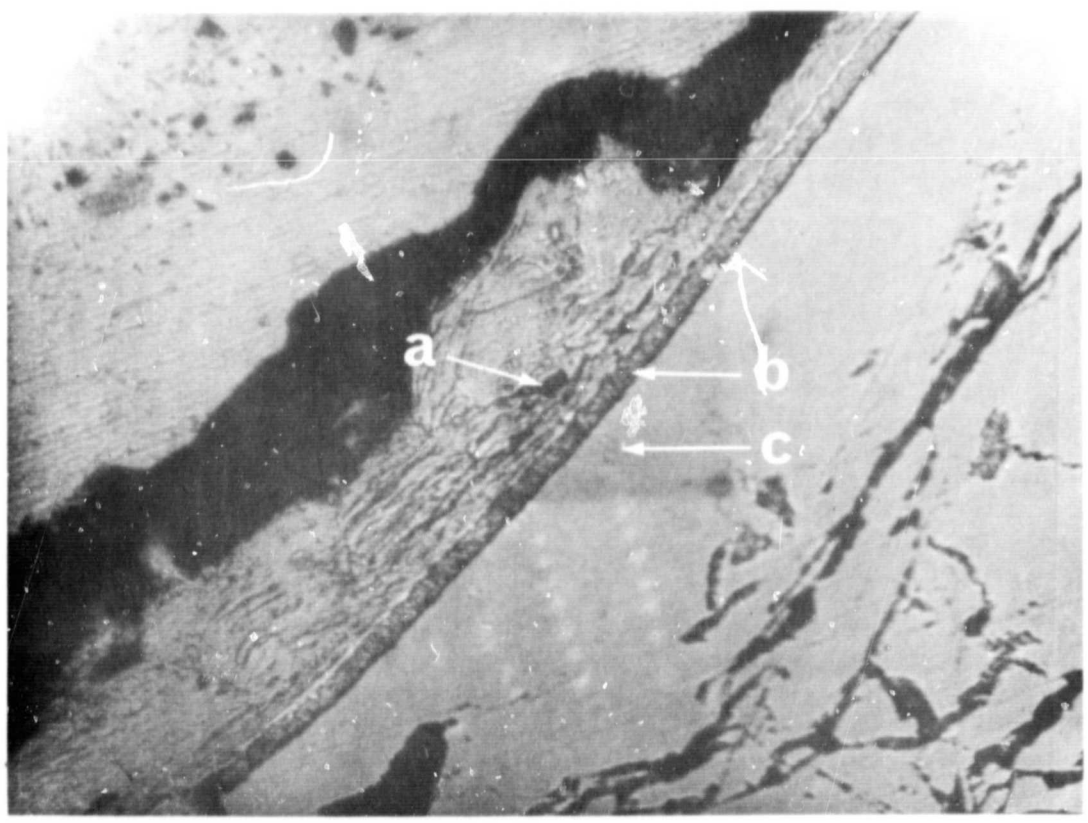

Fig. 3 - Section P1-3D. Pahoehoe lava. Enlarged photomicrograph of the area where electron probe scanning photographs figures 9-13 were taken. Outer band (a) and inner band (b) are similar to area shown in figure 2 but section has been rotated 180°. Matrix (c) is at the bottom. x160

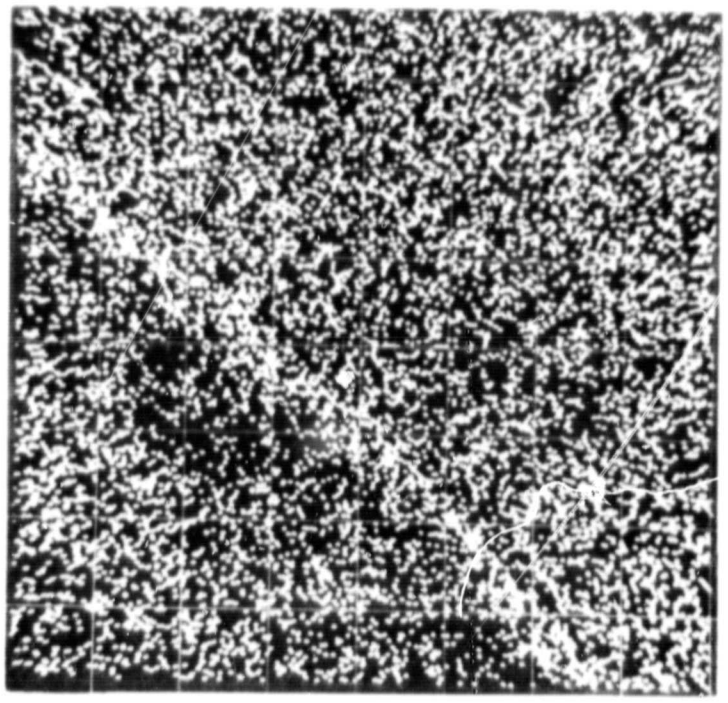

Fig. 4 - Section P1-3D. Pahoehoe lava. Pisgah Flows, San Bernardino County, California. X-ray scanning photograph showing concentrations of Fe.

Top - Matrix
Band - Inner band
Bottom - Outer band

Mag 6 Li F Crystal
25 Kv Fe X-rays
Approximately x450

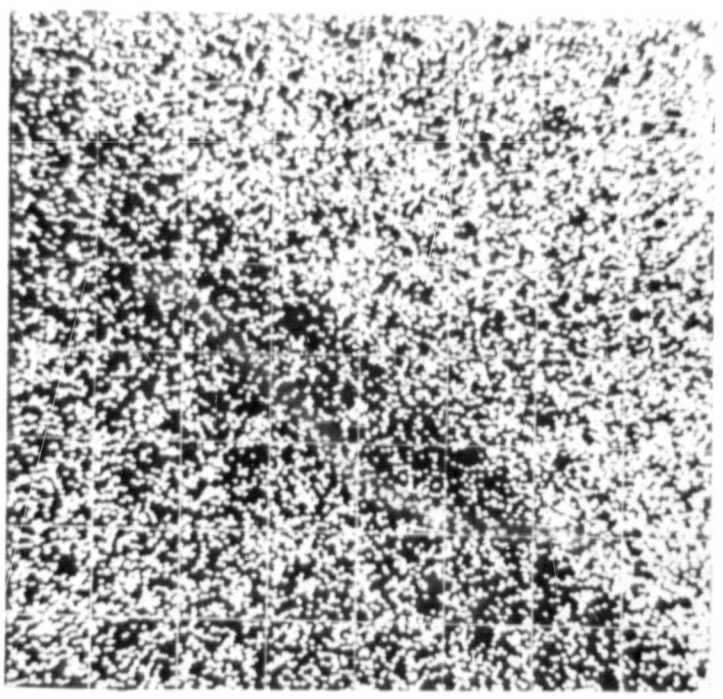

Fig. 5 - Section P1-3D. Pahoehoe lava. Pisgah Flows, San Bernardino County, California. X-ray scanning photograph showing concentrations of Si.

Top - Matrix
Band - Inner band
Bottom - Outer band

Mag 6 KAP Crystal
25 Kv Si X-rays
Approximately x450

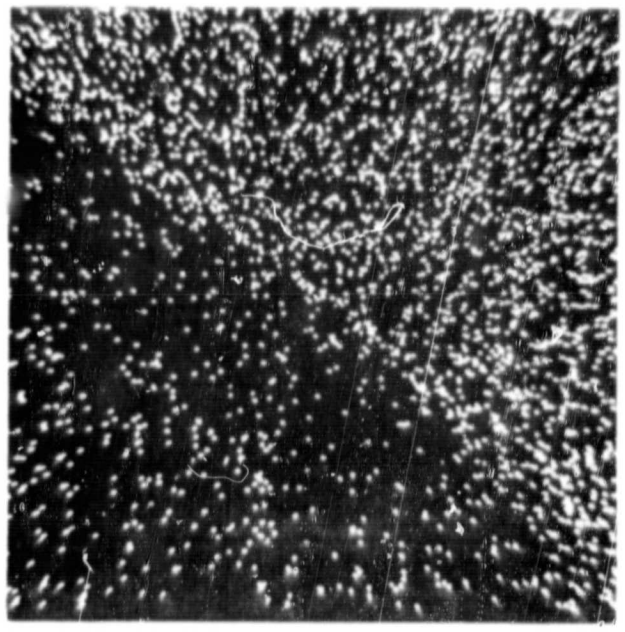

Fig. 6 - Section P1-3D. Pahoehoe lava. X-ray scanning photograph showing concentrations of Al.

Top - Matrix
Band - Inner band
Bottom - Outer band

Mag 6 KAP Crystal
25 Kv Al X-rays
Approximately x450

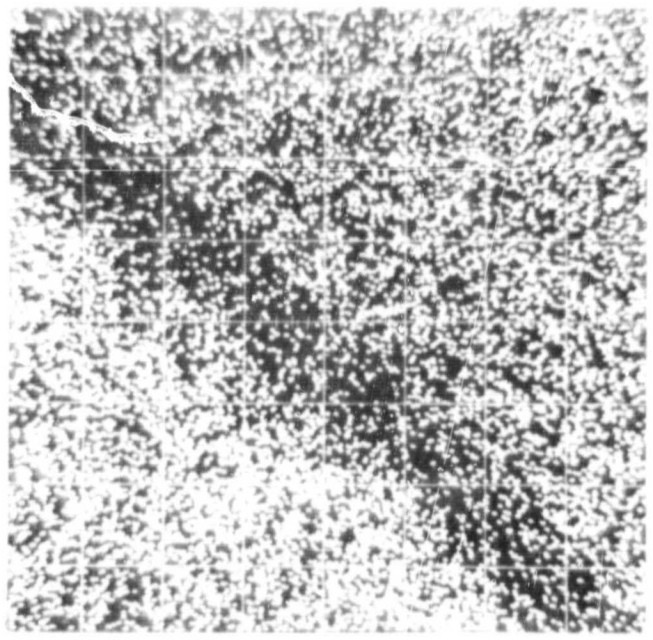

Fig. 7 - Section P1-3D. Pahoehoe lava. X-ray scanning photograph showing concentrations of Ti.

Top - Matrix
Band - Inner band
Bottom - Outer band

Mag 6 LiF Crystal
25 Kv Ti X-rays
Approximately x450

Covers nearly same area as figures 4, 5 and 6, and same area as figure 8.

Fig. 8 - Section P1-3D, Pahoehoe lava. Specimen current photograph showing concentrations of elements of high atomic number as light areas; concentrations of elements of low atomic number are shown as dark areas.

Top - Matrix
Band - Inner band
Bottom - Outer band

Mag 6
25 Kv Picture
Approximately x450

Covers same area as figure 7, nearly same area as figures 4, 5 and 6.

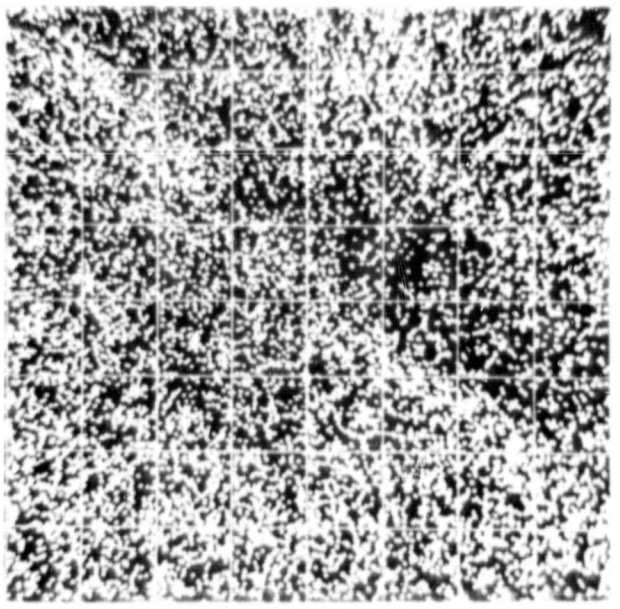

Fig. 9 - Section P1-3D.Pahoehoe lava. X-ray scanning photograph showing concentrations of Fe.

Top - Outer band
Band - Inner band
Bottom - Matrix

Mag 6 Li F Crystal
25 Kv Fe X-rays
Approximately x450

Same general area as figures 4-8, but specimen rotated 180°.

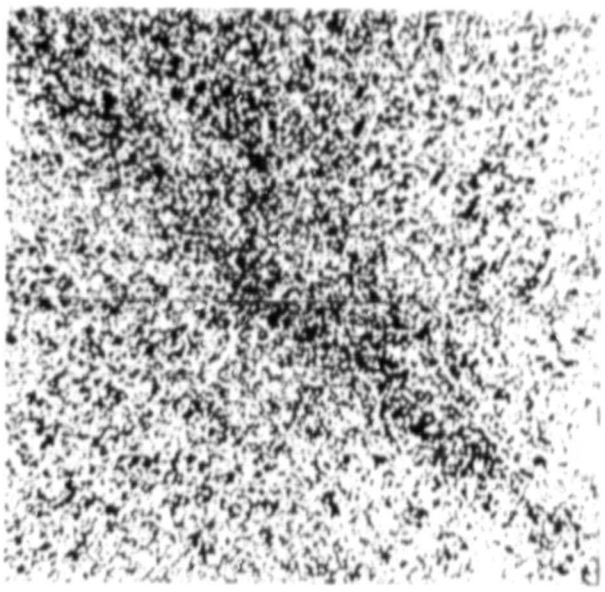

Fig. 10 - Section P1-3D. Pahoehoe lava. X-ray scanning photograph showing concentrations of Si. Same area as figure 9 but specimen rotated 180°.

Si X-rays KAP Crystal Approximately x450

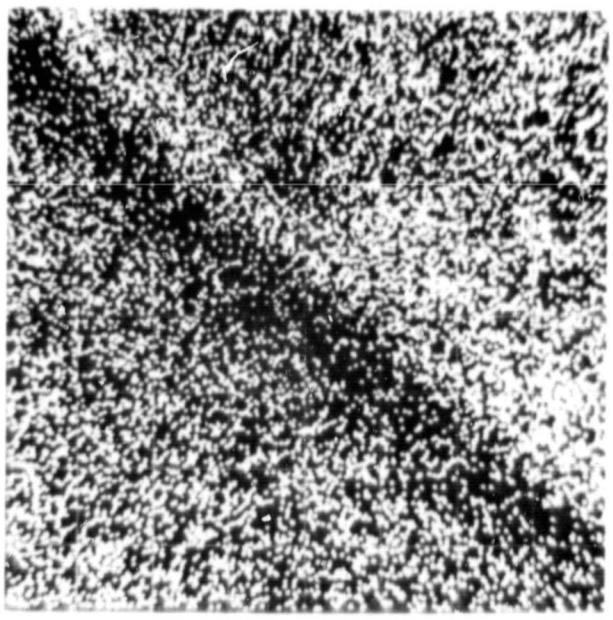

Fig. 11 - Section P1-3D. Pahoehoe lava. X-ray scanning photograph showing concentrations of Al. Same area as figure 9 but specimen rotated 180°.

Al X-rays KAP Crystal Approximately x450

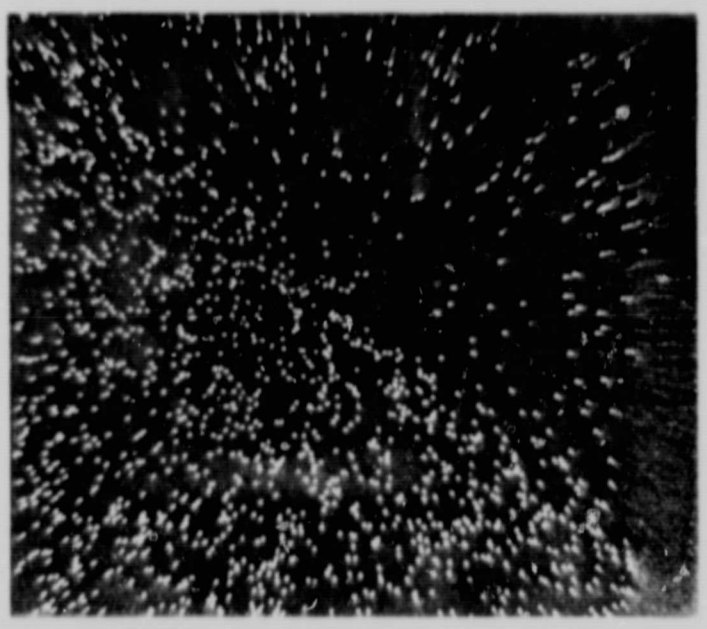

Fig. 12 - Section P1-3D. Pahoehoe lava. X-ray scanning photograph showing concentrations of Ti. Same area as figure 9 but specimen rotated 180°.

Ti X-rays LiF Crystal Approximately x450

Fig. 13 - Section P1-3D. Pahoehoe lava. Specimen current photograph showing concentrations of elements of high atomic number as light areas and concentrations of elements of low atomic number as dark areas. Same area as figure 9 but specimen rotated 180°.

Approximately x450

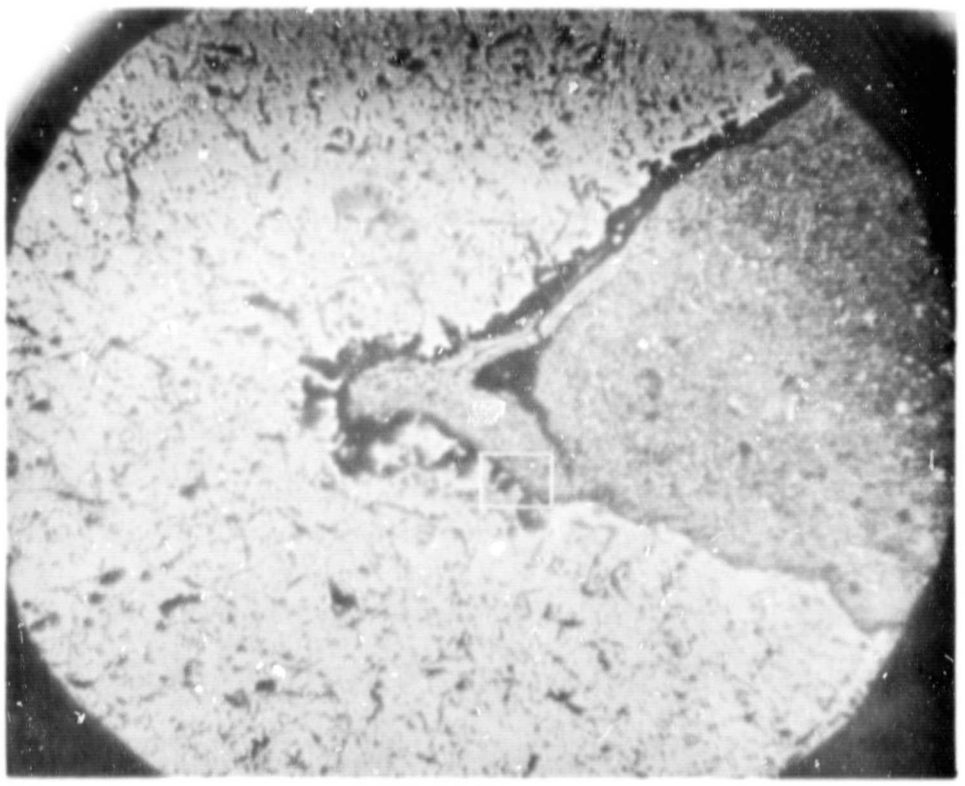

Fig. 14 - Photomicrograph of section P2-3B (aa lava, Pisgah flows, San Bernardino County, California) showing the area included in scanning photographs, figures 16-19. x42

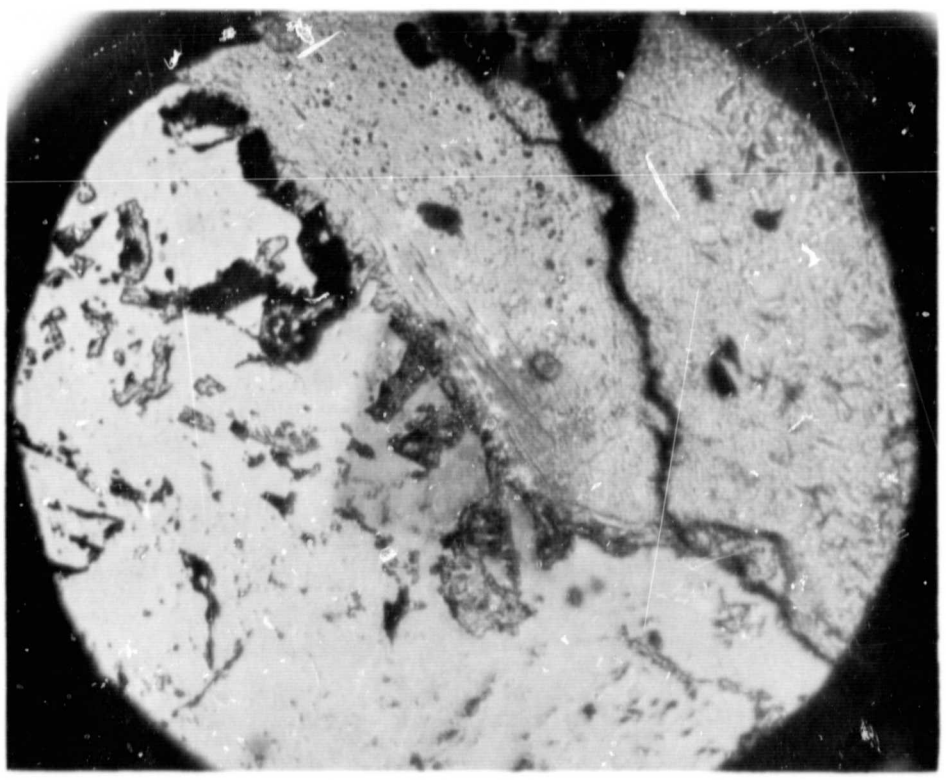

Fig. 15 - Enlarged photomicrograph of section P2-3b (aa) showing the area included in scanning photographs, figures 16-19. x160

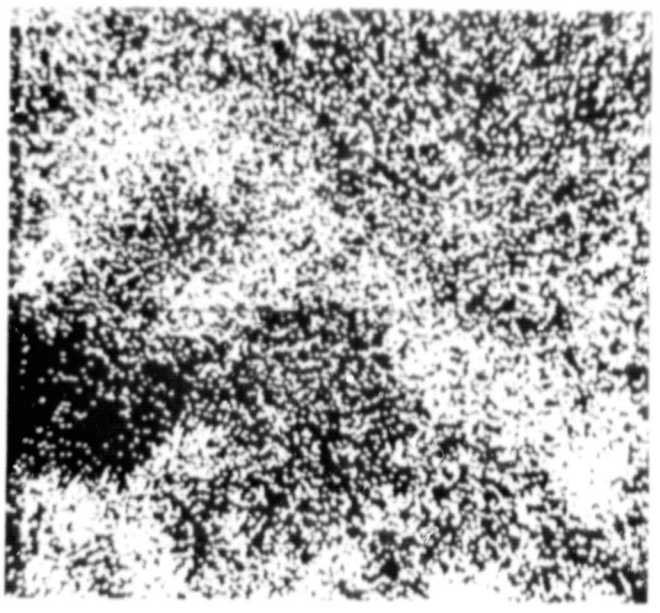

Fig. 16 - Section P2-3b. aa lava. X-ray scanning photograph showing concentrations of Fe.

Top - Outer band
Band - Inner band
Bottom - Matrix

Fe X-rays LiF Crystal
Mag 6
25 Kv
Approximately x450

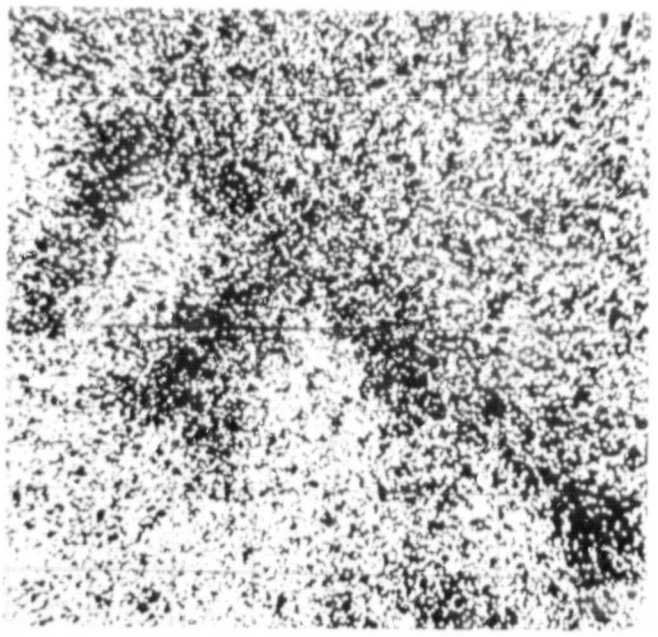

Fig. 17 - Section P2-3B. aa lava. X-ray scanning photograph showing concentrations of Si. Same area as figure 16.

Si X-rays KAP Crystal

Approximately x450

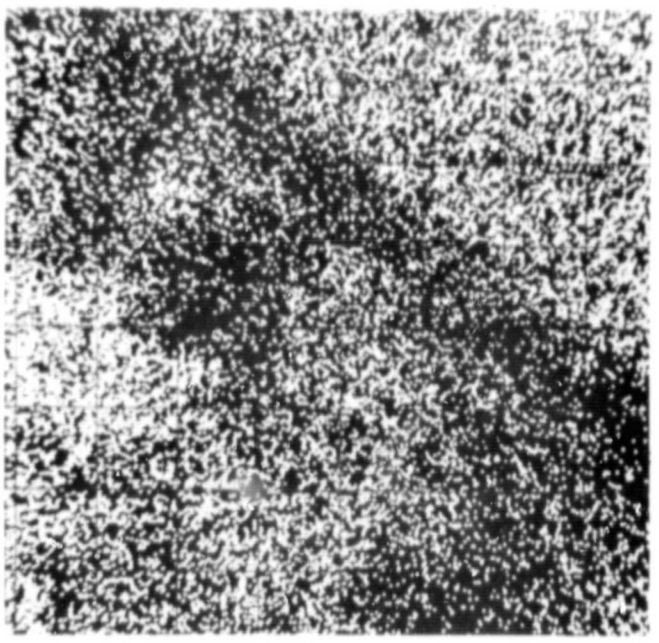

Fig. 18 - Section P2-3b. aa lava. X-ray scanning photograph showing concentrations of Al. Same area as figure 16.

Al X-rays KAP Crystal Approximately x450

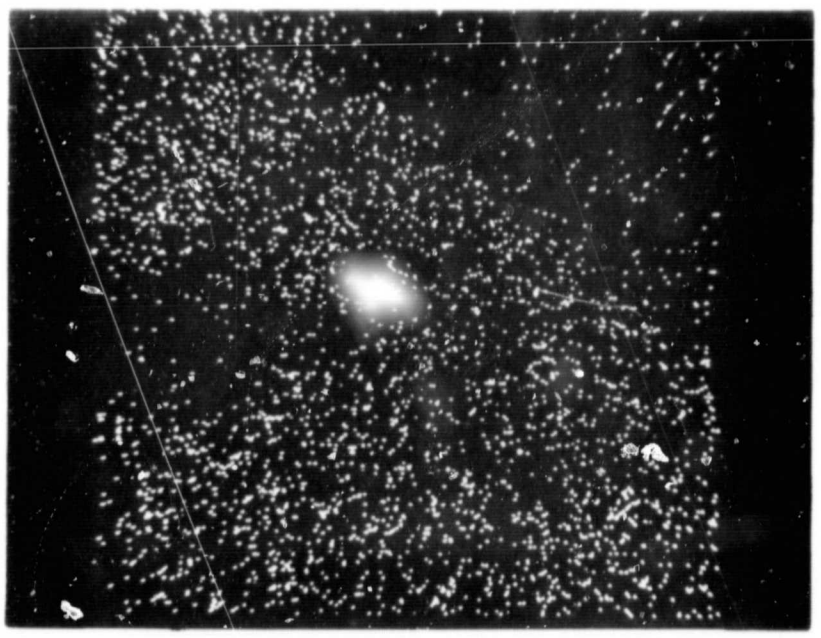

Fig. 19 - Section P2-3b. aa lava. X-ray scanning photograph showing concentrations of Ti. Same area as figure 16.

Ti X-rays LiF Crystal Approximately x450

TABLE 2 SAMPLE PREPARATION

Field No.		Rock Sample	Treatment
P2-3B	(1)	Original sample:	Slices of original, roughly representative of whole sample, ground to powder and mixed.
Porphyritic olivine basalt of eruptive phase two (aa).	(2)	Fresh material chemically freed from fill material:	Fill material chemically removed by alternating treatments with HF and HCL. Residue-washed with water and acetone and then air-dried at room temperature. Residue ground and mixed.
	(3)	Fresh material - hand picked:	Slices free from surface material were gently crushed in a diamond mortar. Representative material essentially free from fill material were selected under the microscope.
	(4)	Vesicle filling material:	The fill material was freed by agitation of rock with acetone. The fill was separated by decantation and air dried and sieved to remove unweathered particles.
	(5)	Surface section:	Thin slices taken as near the surface as possible selected to contain minimum fill material.
P1-3D	(1)	Original sample:	Slices of original, roughly representative of whole sample, ground to powder and mixed.
Porphyritic olivine basalt of eruptive phase three.	(2)	Fresh material chemically freed from fill material:	Fill material chemically removed by alternating treatments with HF and HCL. Residue washed with water and acetone and then air-dried at room temperature. Residue ground and mixed.
P1-3D	(3)	Fresh material - hand picked:	Slices free from surface material were gently crushed in a diamond mortar. Representative material essentially free from fill material were selected under the microscope.
	(4)	Vesicle filling material:	The fill material was freed by agitation of rock with acetone. The fill was separated by decantation and air-dried and sieved to remove unweathered particles.
	(5)	Surface section:	Thin slices taken as near the surface as possible selected to contain minimum fill material.

TABLE 3 MAJOR ELEMENTS BY RAPID ROCK ANALYSIS[1/]

(Rapid Rock Analyses by Paul Elmore, Sam Botts & Lowell Artis)

Aa-textured porphyritic olivine basalt of eruptive phase two.

Field No.	P2-3B1	P2-3B2	P2-3B3	P2-3B4	P2-3B5
SiO_2	47.5	48.3	47.8	50.3	47.6
Al_2O_3	16.9	16.7	17.1	19.0	17.1
Fe_2O_3	2.8	2.8	2.1	5.8	2.8
FeO	7.1	6.6	7.7	1.8	7.1
MgO	7.5	7.7	7.2	3.9	7.7
CaO	9.4	9.0	9.3	5.1	8.9
Na_2O	3.4	3.5	3.7	1.8	3.7
K_2O	1.5	1.4	1.6	2.2	1.5
H_2O-	.20	.45	.00	2.6	.04
H_2O+	.86	.84	.68	5.2	.74
TiO_2	2.1	1.9	2.1	1.3	2.1
P_2O_5	.53	.53	.55	.52	.53
MnO	.18	.16	.15	.18	.19
CO_2	.19	.06	*	*	.08
Sum	100	100	100	100	100

1/ USGS Report N. 65 WRC 87: Job No. 7316: Lot No. 5060 - Methods used were similar to those described in Shapiro and Brannock, 1962.

* Insufficient sample material.

TABLE 3 (CON'T) MAJOR ELEMENTS BY RAPID ROCK ANALYSIS[1/]

Pahoehoe-textured porphyritic olivine basalt of eruptive phase three.

Field No.	P1-3D1	P1-3D2	P1-3D3	P1-3D4	P1-3D5
SiO_2	49.4	50.0	49.7	56.9	49.9
Al_2O_3	17.2	16.9	16.9	16.5	16.6
Fe_2O_3	2.3	2.1	1.8	5.0	3.0
FeO	7.7	7.7	8.8	1.4	6.9
MgO	5.4	5.7	6.0	3.1	5.5
CaO	9.7	9.4	9.5	3.8	9.3
Na_2O	3.3	3.4	3.3	2.3	3.2
K_2O	1.1	1.1	1.0	2.6	1.1
H_2O-	.34	.37	*	2.8	.39
H_2O+	.98	.66	*	3.8	1.1
TiO_2	1.9	1.8	1.9	.98	1.8
P_2O_5	.41	.37	.39	.34	.42
MnO	.18	.16	.16	.11	.20
CO_2	.29	.08	*	.31	.36
Sum	100	100	99	100	100

1/ USGS Report N. 65 WRC 87: Job No. 7316: Lot No. 5060 - Methods used were similar to those described in Shapiro and Brannock, 1962.

* Insufficient sample material.

TABLE 4 DIFFERENCES IN CONTENT BETWEEN SURFACE SECTION AND FRESH MATERIAL

	P2		P1	
	Difference	Percent	Difference	Percent
SiO_2	-0.2	-0.4%*	+0.2	+0.4%**
Al_2O_3	0.0	0.0%*	-0.3	-18.1%**
Fe_2O_3	+0.7	+25.0%**	+1.2	+60.0%**
FeO	-0.6	-8.5%**	-1.9	-21.5%**
MgO	+0.5	+15.4%	-0.5	-8.3%
CaO	-0.4	22.3%	-0.2	-21.0%
Na_2O	0.0	0.0%	-0.1	3.0%
K_2O	-0.1	-15.0%	+0.1	+10.0%
H_2O	+0.06	+0.1%	?	-
H_2O+	+0.06	+8.1%	?	-
TiO_2	0.0	0.0%*	-0.1	-5.3%
P_2O_5	-0.02	-3.7%	+0.03	+7.7%
MnO	+0.04	+21.0%	+0.04	+25.0%
CO_2	?	-	?	-

* Inconsistent with electron probe analysis

** Consistent with electron probe analysis

TABLE 5 Fe_2O_3/FeO ratios

Aa-textured porphyritic olivine basalt of eruptive phase two.		Pahoehoe-textured porphyritic olivine basalt of eruptive phase three.	
Field No.		Field No.	
P2-3B1	0.39	P1-3D1	0.30
P2-3B2	0.42	P1-3D2	0.27
P2-3B3	0.27	P1-3D3	0.13
P2-3B4	3.20	P1-3D4	3.50
P2-3B5	0.39	P1-3D5	0.44
P2-3B means (excluding P2-3B4)	0.38	P1-3D means (excluding P1-3D4)	0.28

TABLE 6 SEMIQUANTITATIVE SPECTROGRAPHIC ANALYSIS

(Analyst Joseph L. Harris)

Results are reported in percent to the nearest number in the series 1, 0.7, 0.5, 0.3, 0.2, 0.15, and 0.1, etc., which represent approximate midpoints of group data on a geometric scale. The assigned group for semiquantitative results will include the quantitative value about 30% of the time.

These data should not be quoted without stating these limitations.

Symbols used are: 0 - looked for but not detected

\- - not looked for

< - with number, less than number shown--here usual detectabilities do not apply

U.S.G.S. Lot No. 5060 Spec. Lab. No. 4158 Plate No. 3578

Aa-textured porphyritic olivine basalt of eruptive phase two.

Field No.	P2-3B(1)	P2-3B(2)	P2-3B(3)	P2-3B(4)	P2-3B(5)
Si					
Al					
Fe					
Mg					
Ca					
			SEE TABLE 2		
Na					
K					
Ti					
P					
Mn					
Ag	<.0001	<.0001	<.0001	<.0001	<.0001
As	0	0	0	0	0
Au	0	0	0	0	0
B	.03	.003	0	0	0
Ba	.05	.03	.03	.05	.03
Be	.00015	.0001	.0001	.00015	.00015
Bi	0	0	0	0	0
Cd	0	0	0	0	0
Ce	.01	.01	.01	.01	.01
Co	.007	.005	.007	.0015	.007
Cr	0	0	0	0	0
Cu	.005	.01	.005	.01	.005
Ga	.0015	.0015	.0015	.0015	.0015
Ge	0	0	0	0	0
Hf	0	0	0	0	0

TABLE 6 SEMIQUANTITATIVE SPECTROGRAPHIC ANALYSIS (CON'T)

Field No.	P2-3B(1)	P2-3B(2)	P2-3B(3)	P2-3B(4)	P2-3B(5)
Hg	0	0	0	0	0
Ln	0	0	0	0	0
La	.005	.005	.007	.007	.005
Li	0	0	0	0	0
Mo	0	0	0	0	0
Nb	.002	.002	.0015	.001	.0015
Ni	.015	.015	.01	.005	.01
Pb	0	0	0	0	0
Pd	0	0	0	0	0
Pt	0	0	0	0	0
Re	0	0	0	0	0
Sb	0	0	0	0	0
Sc	.003	.003	.003	.0015	.003
Sn	0	0	0	0	0
Sr	.1	.07	.07	.03	.07
Ta	0	0	0	0	0
Te	0	0	0	0	0
Th	0	0	0	0	0
Tl	0	0	0	0	0
U	0	0	0	0	0
V	.02	.015	.02	.01	.02
W	0	0	0	0	0
Y	.003	.003	.003	.003	.003
Yb	.0003	.0003	.0003	.0003	.0003
Zn	0	0	0	0	0
Zr	.03	.02	.03	.015	.03
Looked for only when La or Ce found:					
Pr	0	0	0	0	0
Nd	0	0	0	0	0
Sm	0	0	0	0	0
Eu	0	0	0	0	0
Looked for only when Y is found above .005%					
Gd	-	-	-	-	-
Tb	-	-	-	-	-
Dy	-	-	-	-	-
Ho	-	-	-	-	-
Er	-	-	-	-	-
Tm	-	-	-	-	-
Lu	-	-	-	-	-
Looked for only when Pd or Pt found:					

TABLE 6 SEMIQUANTITATIVE SPECTROGRAPHIC ANALYSIS (CON'T)

Field No.	P2-3B(1)	P2-3B(2)	P2-3B(3)	P2-3B(4)	P2-3B(5)
Lr	-	-	-	-	-
Os	-	-	-	-	-
Rh	-	-	-	-	-
Ru	-	-	-	-	-
Looked for only when requested:					
Cs	-	-	-	-	-
Rb	-	-	-	-	-
F	-	-	-	-	-

Pahoehoe-textured porphyritic olivine basalt of eruptive phase three.

Field No.	P1-3D(1)	P1-3D(2)	P1-3D(3)	P1-3D(4)	P1-3D(5)
Si					
Al					
Fe					
Mg					
Ca					
		SEE TABLE 2			
Na					
K					
Ti					
P					
Mn					
Ag	<.0001	<.0001	<.0001	<.0001	<.0001
As	0	0	0	0	0
Au	0	0	0	0	0
B	0	0	0	0	0
Ba	.03	.03	.03	.05	.03
Be	.0001	.0001	.0001	.00015	.0001
Bi	0	0	0	0	0
Cd	0	0	0	0	0
Ce	.01	.01	.01	.02	.02
Co	.005	.005	.005	.001	.001
Cr	.03	.03	.03	.01	.03
Cu	.007	.007	.007	.007	.007
Ga	.0015	.0015	.0015	.002	.002
Ge	0	0	0	0	0
Hf	0	0	0	0	0

TABLE 6 SEMIQUANTITATIVE SPECTROGRAPHIC ANALYSIS (CON'T)

Field No.	P1-3D(1)	P1-3D(2)	P1-3D(3)	P1-3D(4)	P1-3D(5)
Hg	0	0	0	0	0
Ln	0	0	0	0	0
La	.005	.005	.005	.007	.005
Li	0	0	0	0	0
Mo	0	0	0	0	0
Nb	.001	.001	.001	0	.001
Ni	.003	.005	.005	.003	.005
Pb	0	0	0	0	0
Pd	0	0	0	0	0
Pt	0	0	0	0	0
Re	0	0	0	0	0
Sb	0	0	0	0	0
Sc	.003	.003	.003	.0015	.003
Sn	0	0	0	0	0
Sr	.05	.05	.05	.03	.05
Ta	0	0	0	0	0
Te	0	0	0	0	0
Th	0	0	0	0	0
Tl	0	0	0	0	0
U	0	0	0	0	0
V	.02	.02	.02	.01	.02
W	0	0	0	0	0
Y	.003	.003	.003	.003	.003
Yb	.0003	.0003	.0003	.0003	.0003
Zn	0	0	0	0	0
Zr	.02	.02	.02	.03	.02
Looked for only when La or Ce found:					
Pr	0	0	0	0	0
Nd	0	0	0	0	0
Sm	0	0	0	0	0
Eu	0	0	0	0	0
Looked for only when Y is found above .005%:					
Gd	–	–	–	–	–
Tb	–	–	–	–	–
Dy	–	–	–	–	–
Ho	–	–	–	–	–
Er	–	–	–	–	–
Tm	–	–	–	–	–
Lu	–	–	–	–	–
Looked for only when Pd or Pt found:					
Lr	–	–	–	–	–
Os	–	–	–	–	–
Rh	–	–	–	–	–
Ru	–	–	–	–	–
Looked for only when requested:					
Cs	–	–	–	–	–
Rb	–	–	–	–	–
F	–	–	–	–	–

CONCLUSIONS

1) Major and minor element composition of eruptive phase two (porphyritic olivine basalt flow) and eruptive phase three (porphyritic olivine basalt flow) are similar. The older flow may be slightly more sodic and the younger flow slightly more calcalkalic. Major element composition of surface sections of both flows indicates surface enrichment in Fe_2O_3 and possibly in M_nO and depletion of FeO; there are suggestions of a greater Fe_2O_3/FeO ratio in phase two than in phase three.

2) Photomicrography and electron probe microanalysis indicate the presence of two surface layers 15μ to 150μ thick and also suggest surface enrichment in Fe_2O_3.

3) It is suggested that these surface layers are a form of desert varnish resulting from movement of iron and manganese to the surface by capillary action. The process may have occurred more extensively in the aa flow (phase two) than in the pahoehoe (phase three) for two reasons:

   a) The aa has a greater surface-to-volume ratio (Fischer 1965, fig. 9) and

   b) it is older.

4) The vesicle fill material and surface dust has definite wide-ranging differences in composition from the basalts in both major and minor elements. At least some of this material is eolian sand and silt; some of it must also be the product of weathering and erosion of the basalt.

5) The geologic implications of differences between fresh and surface materials noted in the two samples studied could be verified by systematic sampling for compositional analysis and subsequent statistical procedures. A study could be carried out, for example, on the uniformity of the Fe_2O_3/FeO ratio of the aa (phase two) flow in contrast to the pahoehoe (phase three) flow. If the higher Fe_2O_3/FeO ratio reported here persists throughout the phase two flow a useful geologic mapping tool would be available. Moreover, a comparison of the Fe_2O_3/FeO ratio (0.33) of the Pisgah basalts (1000 ± years old) with similar basalts of different ages in arid environments could provide information on the rate of accumulation of desert varnish.

6) Although both $\varepsilon_{8-13\mu}$ and β are partially dependent upon composition, wider deviations resulting from variations in other physical properties (e.g., vesicularity, density, heat capacity) are expected than from variations in chemical composition.

(ε= emissivity; β = thermal inertia, i.e., thermal contact coefficient).

REFERENCES

Altenhofen, R. E., Oman, J. K., and Sousa, T. M., 1965, Topographic Studies of Pisgah Crater, California; Tech. Letter NASA - 7.

Badgley, P. C., and Lyon, R. J. P., 1965, Lunar exploration from orbital altitudes; Geol. Problems in Lunar Research, Annals of New York Acad. Sci., v. 123, art. 2, sec. 10, p. 1198-1219, illus.

Birch, F., and Clark, H., 1940, The thermal conductivity of rocks and its dependence upon temperature and composition; Am. Jour. Sci., v. 238, no. 8, p. 529-558, tables.

Buettner, K. J. K., Kern, C. D., 1965, The determination of infrared emissivities of terrestrial surfaces; Jour. Geophys. Research, v. 70, no. 6, p. 1329-1337.

Carlslaw, H. S., and Jaeger, J. C., 1959, Conduction of heat in solids; Oxford, Clarendon Press, 2nd ed., 510 p.

Fischer, W. A., Friedman, J. D., Sousa, T. M., 1965, Preliminary results of aerial infrared surveys at Pisgah Crater, California; Tech. Letter NASA - 5.

Gawarecki, S. J., 1964, Geologic reconnaissance report of the Pisgah Crater, California Area; Tech. Letter NASA - 2.

Oman, J. K., 196 , Reflectivity of rock samples from Pisgah Crater, San Bernardino County, California (unpub.); Tech. Letter NASA - .

Moxham, R. M., Crandell, D. R., and Marlatt, W. E., 1966, Thermal features at Mount Rainier, Washington, as revealed by infrared surveys; U. S. Geol. Survey Prof. Paper 525-D, p. D93-D100, illus.

Shapiro, Leonard, and Brannock, W. W., 1962, Rapid analysis of silicate, carbonate, and phosphate rocks; Bull. 1144-A, U. S. Geological Survey.

Wise, W. S., 1966, Geologic map of Pisgah and Sunshine Cone lava fields; Tech. Letter NASA - 11.